Modeling green roofs' cooling effect in high-density urban areas based on law of diminishing marginal utility of the cooling efficiency: A case study of Xiamen Island, China

Meixia Lin [a,b], Jing Dong [c], Laurence Jones [d], Jiakun Liu [e], Tao Lin [a,*], Jin Zuo [c,**], Hong Ye [a], Guoqin Zhang [a], Tiejun Zhou [f]

[a] Key Laboratory of Urban Environment and Health, Institute of Urban Environment, Chinese Academy of Sciences, Xiamen, 361021, China
[b] University of Chinese Academy of Sciences, Beijing, 100049, China
[c] School of Architecture, Tianjin University, Tianjin, 300072, China
[d] UK Centre for Ecology and Hydrology, Environment Centre Wales, Bangor, LL57 2UW, UK
[e] Department of Human Geography and Spatial Planning, Faculty of Geosciences, Utrecht University, Utrecht, 3584 CB, Netherlands
[f] Faculty of Architecture and Urban Planning, Chongqing University, Chongqing, 400045, China

ARTICLE INFO

ABSTRACT

There is in general good awareness of the potential role of green roofs to regulate urban thermal environments, but a lack of effective spatial modeling of this cooling effect for a given roof greening scheme at the city scale. This study proposes a simplified and feasible approach to simulate the cooling effect provided by green roofs as a mitigation option to combat urban heat island effects in high-density urban areas. In this study, we established a spatial model of the cooling effect of green roofs, which integrated remote sensing methods and a statistical model based on the law of diminishing marginal utility of the cooling efficiency of green roofs (DMUCE) deduced from previous studies. A case study in Xiamen City, China demonstrates the applicability and implications of the model. Our modeling clearly simulated the size and strength of the urban cool island and its variation under different green roof scenarios. We found that green roofs play an important part in moderating the thermal environment in areas where larger green spaces and waterbodies are largely absent. When the proportion of green roofs is implemented at scale, roofs that are only partly green can also create some extra cool islands (not merely normal islands) in high-density urban areas, equivalent to small green spaces and waterbodies. The sensitivity analysis of the cooling effect indicated that the maximum potential benefit of heat island reduction ranged from 4.04 km^2 to 9.75 km^2 when the coverage of green roofs was extended to the entire Xiamen Island. Besides, our results suggested that all proposed strategies would not remarkably moderate the thermal environment in the north of Xiamen Island, where urban planners should pay more attention in the future.

1. Introduction

The urban heat island effect is one of the most typical urban environmental issues threatening human health and urban sustainability (Akbari and Kolokotsa, 2016; Yin et al., 2019b). The formation of the urban heat island phenomenon in cities is contributed by several factors, and lack of urban vegetation is one of the factors leading to the increase of urban temperature (Grimm et al., 2008; Zhou et al., 2011). Urban greening has been proved to alleviate the adverse impacts of increased temperatures resulting from urbanization and climate change (Yu and Hien, 2009; Bowler et al., 2010; Wang et al., 2015). Extensive studies found that green urban infrastructure (GUI, e.g. parks, greenspaces, trees, water bodies, and ground or roof-top vegetation) proposed as one approach to bring nature back into cities and make cities re-green, can not only strengthen the resilience of cities to heat waves and extreme temperature (Zardo et al., 2017) but can also effectively improve public health and human well-being (Gascon et al., 2015). However, with more people inhabiting cities, a greater proportion of the land is exploited for residential, commercial, industry and other public utilities (Lin et al., 2020; Liu et al., 2020), leaving limited space for urban greening.

In recent years, mitigation strategies in regard to urban rooftops have been increasingly emphasized (Gagliano et al., 2015)and the implementation of green roofs is regarded as a cost-effective nature-based solution (NBS) to increase urban vegetation and create cooling spaces, especially in high-density urban areas (HDUA) (Faivre et al., 2017; Liu et al., 2019). Moreover, it provides a range of potential co-benefits, such as improving aesthetic of rooftops (Ferguson, 2012), retaining stormwater (Yilmaz et al., 2016), removing air pollutant (Karteris et al., 2016), reducing energy consumption (Ziogou et al., 2017; Zinzi and Agnoli, 2012), providing potential habitats for insects and birds, and an alternative land for food production (Demuzere et al., 2014). Urban areas will receive more cooling benefits when mitigation strategies are performed at a larger scale (Ouyang et al., 2020; Santamouris, 2014). Nevertheless, such upscaling strategies must be cost-effective if they expect to be approved by stakeholders and decision-makers. Therefore, it is essential to assess the implementation potential of roof greening and estimate its cooling efficiency at the city level prior to any interventions. Yet, to our knowledge, urban planners usually pay more attention to evaluating the implementation potential and suitability of urban rooftops, but overlooking the overall cooling effect of the deployment scheme of green roofs, which would enable urban planners to optimize roof greening planning and exert its maximum ecological benefits (Takane et al., 2019).

The cooling capacity and mechanisms of green roofs have been studied worldwide at various scales (micro-, local- and meso-scale) mainly by using three different methods, including field experimentation (Lin et al., 2013; Bevilacqua et al., 2017), numerical studies and a combination of laboratory or field experiments with numerical models (Ng et al., 2012; Olivieri et al., 2013). Although these attempts focusing on measuring and modeling the cooling capacity of green roofs provide better knowledge for urban planners to estimate the cooling efficiency at a single site, to evaluate the benefits and the temperature reduction in response to the broader roof greening can only resort to simulations. To date, comprehensive climate models and land surface temperature inverted from remote sensing images have been widely used to simulate the thermal environment at larger scale. In general, comprehensive climate models can be used to predict the thermal effects of green roofs at building scale and city scale (Karteris et al., 2016), e.g. three-dimensional microclimate model ENVI-met 4.2 (Jiang et al., 2018; Shen et al., 2017), and the Advanced Research version of the Weather Research and Forecasting Model (http://www.wrf-model.org/index.php) coupled with an urban canopy model (WRF-UCM) (Smith and Roebber, 2011). These models can produce more accurate simulation results and shed light on landscape heterogeneity and land-atmosphere interactions, but they are highly parameterized, and to run them usually requires a series of long list of input parameters and datasets, including meteorological data, urban canopy, detailed biophysical attributes of vegetation of green roofs, hydrological and thermal properties of each land cover type, etc. (Yang and Bou-Zeid, 2019). A reliable prediction strongly depends upon the accuracy and quality of the input data used in the models. However, processing these data and operating professional models generally go beyond the know-how of most urban planners.

Meanwhile, evidence has suggested that remote sensing can provide much of the information required to assess the benefits of green roofs. One technique is a rapid and effective method to invert land surface temperature (LST) and examine the reduction of LST resulting from the influence of vegetation on a large scale (Phelan et al., 2015; Shen et al., 2016). Compared with climate model simulations, a remote sensing method is easier to operate and the data needed is more accessible. For instance, Sun et al. (2012) and Yu et al. (2017) utilized Landsat 8 satellite imagery to invert the LST of study areas and to calculate the temperature difference between GUI and its buffer zones, determining the cooling effect, maximum cooling distance and cooling efficiency of GUI. However, this method is more suitable for post-fact assessment because we cannot obtain corresponding satellite imageries before green roof plans implemented.

Given all the above, it is necessary to come up with a more feasible approach with less input data to provide a spatial simulation of the cooling effect for a given green roof planning and design in high-density urban areas. Here we propose a quantitative method to simulate the cooling effect generated by green roofs in HDUA. The main objectives of this study are to: i) simulate the thermal environment of a given roof greening scenario ii) quantify the spatial variation of the cooling effects of diverse roof greening plans; iii) apply the approach to an illustrative case study in the HDUA.

2. Study area

Xiamen City (24°23′-24°54′N, 117° 53′-118°26′E) is located in Fujian Province of southeastern China (Fig. 1), which belongs to subtropical marine monsoon zone with a mild and rainy climate. The annual precipitation is approximately 1513.3 mm (1956–2015) and the average monthly temperature ranges from 13 to 28 °C. Xiamen has experienced the transformation from an island city to a bay city since the beginning of the 1980s. The urbanization ratio of Xiamen raised up from 35% in 1980 to 89.1% in 2017, meanwhile the construction land area expanded from 12 km² in 1981 to 364 km² in 2017. The rapid demographic and urban growth led to the development of an intense urban heat island (UHI) (Zhao et al., 2010), with the spatial extent of UHI continuously expanding with the urban sprawl from the urban center on the island to the suburban areas in the bay.

Xiamen Island was chosen as a case study area (Fig. 1). It is not only the urban core area with a total area of 142 km², but also typical of the high-density built-up areas of the city with a population density of approximately 16,700 people/km² in 2017. Although it was reported that UHI in the partially built-up area was alleviated as a result of urban renewal and growing greenery, especially in the old urban area on the island (Sun et al., 2019), there still exists a series of adverse environmental impacts in Xiamen Island. For instance, UHI reduced the humidity in the urban center of Xiamen and intensified the frequency of extreme rainstorms. The increasing demand for air conditioning in summer due to the high temperature has magnified energy consumption and lowered air quality (Xu and Chen, 2004). Since 2015, Xiamen has been carrying out roof greening as one of the strategies to combat UHI and improve the living environment. Studies revealed that the mean temperature difference between green roofs and the entire study area in 2017 dropped by 0.91 °C compared with that in 2014 (Dong et al., 2020). By 2017, the area of green roofs deployed on Xiamen Island reached 0.54 km², equal to 2% of the rooftop area of Xiamen Island (Fig. 5a). In the next stage, Xiamen will increase the scale of green roofs. It has been confirmed that green roofs can definitively provide cooling benefits. However, the quantitative laws and spatial extent of the cooling benefits from a given roof greening intervention planning remains unknown, and is the focus of this study.

3. Methods and materials

3.1. Overview of the methodology

The framework of the proposed method can be summarized as four steps in Fig. 2. In step 1, we identified the key factors (distance and area) of the cooling effect of green spaces/roofs deduced from literature reviews and our previous empirical study. On this basis, in step 2, we defined the law of diminishing marginal utility of the cooling efficiency of green roofs and established a spatial model of the cooling effect of green roofs, including drawing response curves and constructing formulas. In step 3, taking Xiamen Island as an illustrative study area, we initialized the model and assessed the cooling effects of Xiamen Island with different proportions of green roofs implemented through scenario analysis. Specifically, we determined the key parameters of the spatial model in Section 4.1 from our previous study results and simulated the LST of Xiamen Island under different scenarios, see Fig. 6. Besides,
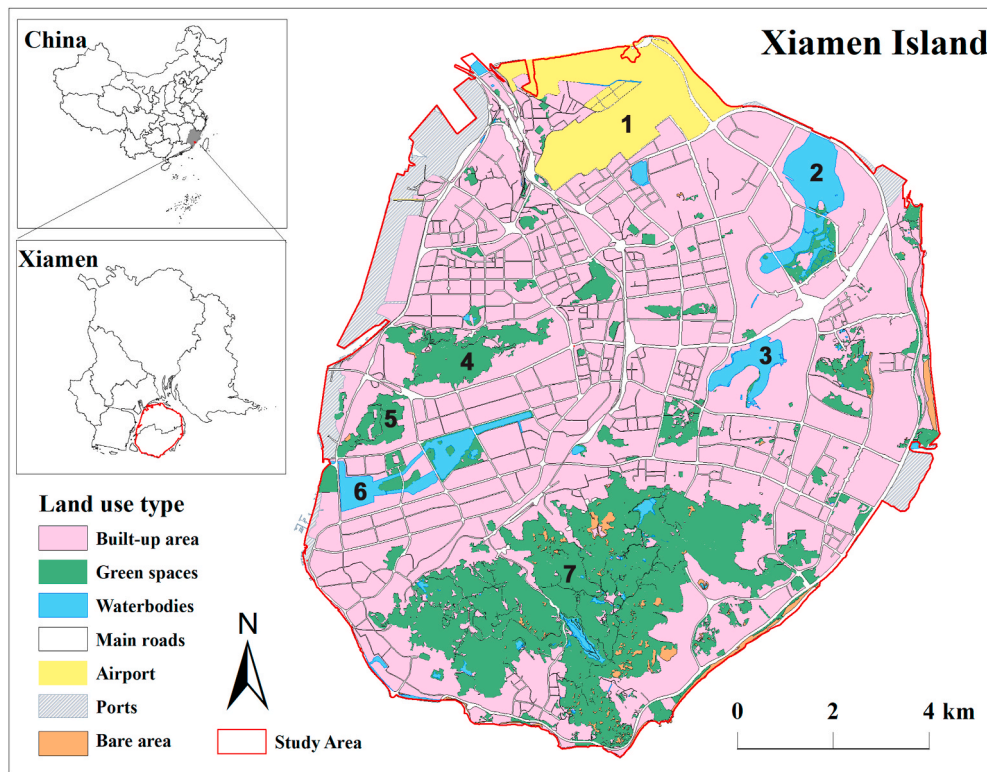
Fig. 1. Location of study Area and land use of Xiamen Island in 2017. (1) Xiamen Gaoqi International Airport, (2) Wuyuan Bay, (3) Hubian Reservoir, (4) Xianyue Park, (5) Mountain Huwei, (6) Yuandang Lake, (7) Mountain Wanshi.
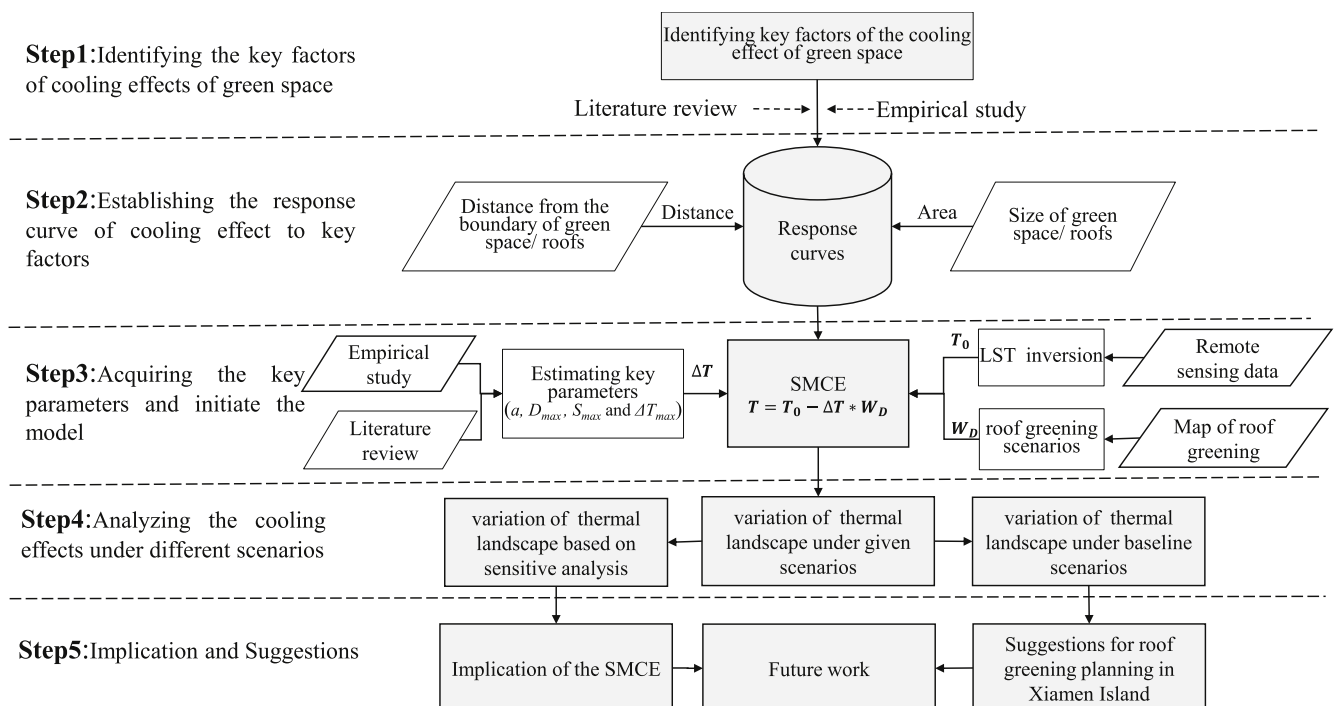

Fig. 2. The framework of the proposed method.

considering the uncertainty of cooling efficiency, we designed optimistic and pessimistic scenarios in Section 4.3 to estimate the maximum and minimum cooling benefits of green roofs. In step 4, we concluded the implications of the model and provided some suggestions for roof greening planning in Xiamen Island in the next stage. Each of these steps

will be discussed in further detail below.

3.2. Literature reviews

Previous studies have proved that the size of green space influences

the magnitude of the LST between green space and its surroundings (defined as the cooling effect) and the spatial extent of cooling effect accords with the law of diminishing marginal utility (Hillevi et al., 1998; Du et al., 2016; Yu et al., 2018; Sun et al., 2012). Yu et al. (2017) delimitated the relationships between the cooling effect of green space and the size of green space and the distance from the green space border as the response curves shown in Fig. 3. Specifically, 1) the bigger size of green space, the larger the cooling extent. Beyond a certain distance, the cooling effect of the central green space will not significantly increase. (Fig. 3a). 2) increasing the area of green space conduces to an increased temperature difference between central green space and its surroundings. However, the temperature difference will not infinitely increase. There is an effective threshold value of the area of green space, at which the cooling effect will keep stable within a certain range (Fig. 3b).

Green roofs, play a critical part in alleviating UHI, as do waterbodies and green spaces in HDUA. Literature reviews revealed that green roofs could directly or indirectly affect the temperature of the buildings (internal) and its surrounding (external) environment mainly via the mechanism of evapotranspiration and shade provided by green vegetation (Santamouris et al., 2017; Arabi et al., 2015). However, it was found that the cooling capacity of green roofs exhibited significant differences in both context and scale dependence. Specifically, the cooling benefits provided by green roofs critically depend on the physical and configurational characteristics of green roofs (e.g. the size and type of vegetation) (Yu et al., 2020b; Zardo et al., 2017), the geo-climatic condition (e. g. wind pattern) and urban canopy of the sites where they will be deployed (Bartesaghi Koc et al., 2018; Lin et al., 2013). Besides, Berardi (2016) proved that the cooling effect of the green roof retrofits of the main Ryerson building was more pronounced at the rooftop level than at the pedestrian level. This may attribute to the influence of building height and it is evident that green roof will exert a different magnitude of cooling effect on its surrounding area and it is obvious that the closer to green roof retrofits, the higher the temperature reduction. Yang and Bou-Zeid (2019) found that the cooling efficiency decreases with the implementation scale of green roofs in six U.S. cities, which accords with an underlying power law function. Dong et al. (2020) indicated that green roofs in Xiamen Island could exert a cooling effect on their ambient environment and the cooling effect of green roofs depends on the size of the central green roof and distance from the central green roof, which is similar to the law of diminishing marginal utility of the cooling effect of green spaces. Based on literature analysis above, we identified the size of the central green roof and distance from the central green roof are two key factors of the cooling effect of green roofs and the relationships between them comply with the law of diminishing

marginal utility. Although it is may not a conclusive scientific rule, it has been widely noticed and proved and it is useful for urban green roof planning and design (Bowler et al., 2010).

3.3. Spatial model construction of green roof cooling effect in HDUA

3.3.1. Definition of the law of diminishing marginal utility of the cooling efficiency

As mentioned above, the cooling capacity of green roofs exhibited significant differences due to various factors, therefore, each green roof theoretically has its own independent response curve. Although it is not possible to obtain a generalizable function to illustrate the relationship between the cooling efficient of green roofs and all its factors, what we clear enough from literature reviews is that the functional relationship between temperature difference and cooling distance can be described as exponential or linear decline and the decline rate depends on the size of green roof (Yang and Bou-Zeid, 2019; Dong et al., 2020). Therefore, in this study, we propose corresponding conceptual response curves to the cooling effect of green roofs illustrated as Fig. 4 and describe it as the law of diminishing marginal utility of the cooling efficiency of green roofs (DMUCE). Specifically, 1) Temperature difference increases with increased green roof area, and at a certain point, the slope of curve changes sharply or reaches a relatively flat level Fig. 4a. 2) The closer to green roof, the lower the ambient temperature is. The cooling effect of green roof diminishes in distance at the border and vanishes at a certain distance, which is denoted as the maximum cooling distance (D_{max}, Fig. 4b–c).

Notably, LST around a green roof within the maximum cooling distance may be influenced by other adjacent green roofs. In this case, the temperature difference at the same spot (e.g., point A in Fig. 4d and point A′ in Fig. 4e) may be larger than that only affected by one single green roof ($\Delta T_1 > \Delta T_2$, in Fig. 4b–c). For instance, supposing the area of green roof S_1 equals S_2, and they have the same cooling capacity (D_{max} and ΔT_{max}), the LST of point A in (Fig. 4d) may be equal or higher than that of same point A′ in (Fig. 4e). Therefore, considering the additional cooling effects from nearby green roofs, we assume that the curve tendencies of the single and the multiple are similar, but the response curve to multiple is always above the counterpart of the single (Fig. 4c–d).

3.3.2. Formulas to quantify the cooling effect of green roofs

Theoretically, the response curve of temperature difference to cooling distance is more intricate than that ideal one described in Fig. 4b-c. The curvatures of those response curves, ΔT_{max}, and D_{max} may vary with the area of green roof and its ambient environment. To determine the
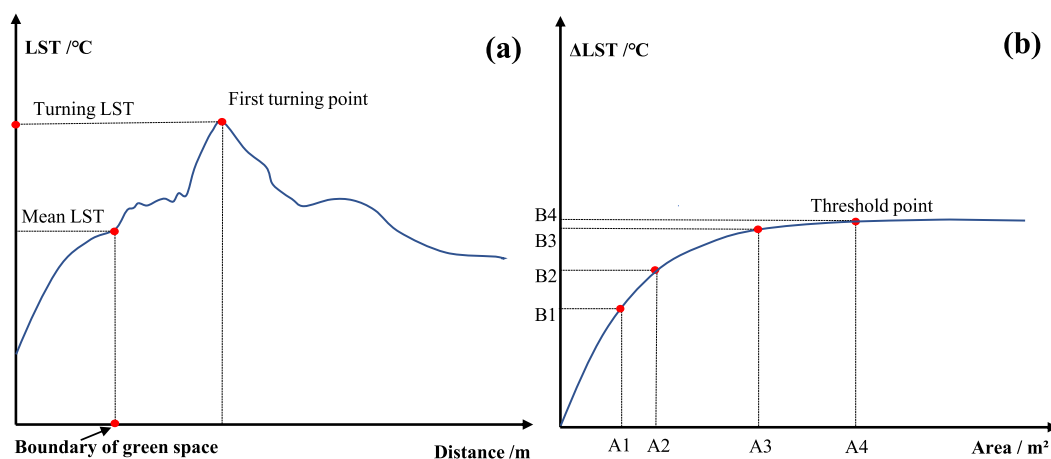

Fig. 3. Response curves to the cooling effect of green space adapted from Yu et al. (2017) (a) illustrates the cooling effect of green space decreased along with the distance from the boundary of green space. (b) illustrates the cooling effect (ΔLST) increased with the size of green space and become stable at the threshold point. The increase of green space area is the same between (A2 -A1) and (A4 -A3), but the ΔLST (B2–B1) is larger than ΔLST (B4–B3). (For interpretation of the references to colour in this figure legend, the reader is referred to the Web version of this article.)
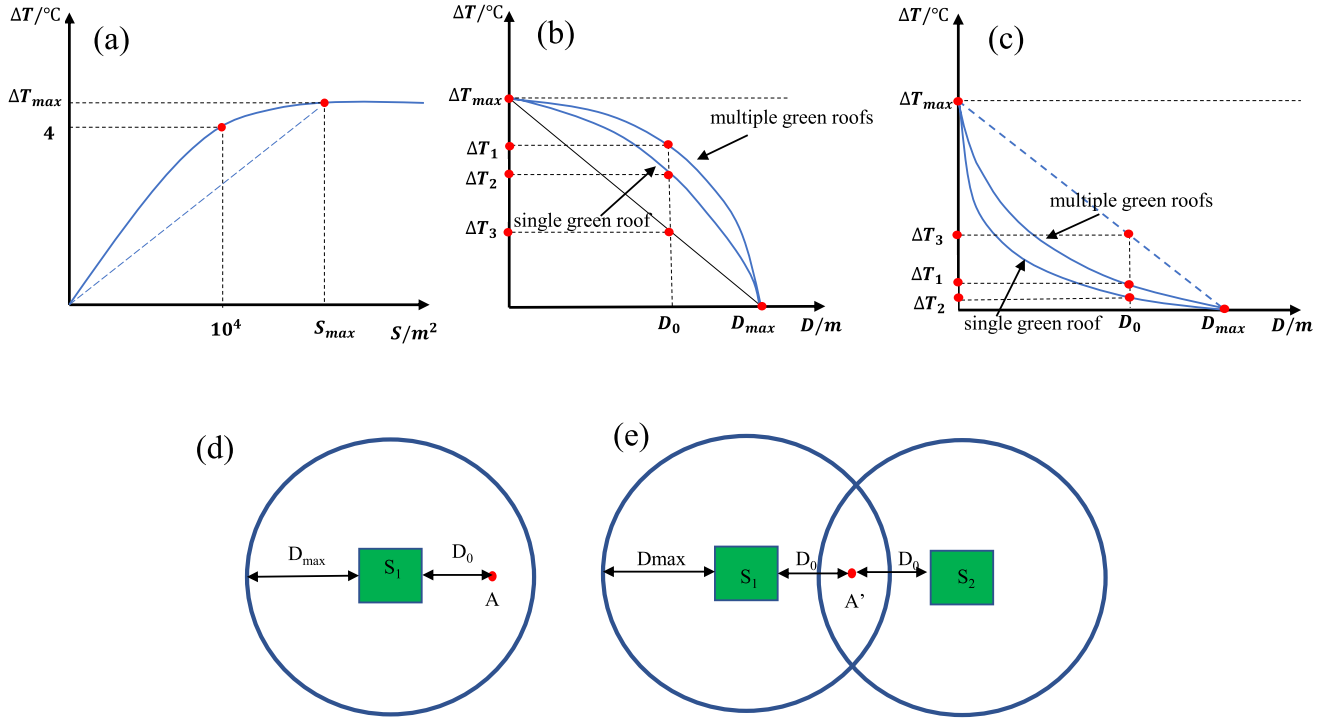
Fig. 4. Conceptual curves of law of diminishing marginal utility of the cooling efficiency of green roofs. (a) describes the response curve of temperature difference ($\Delta T/°C$) to green roof area(S/m^2), the detail figures (4 °C, 10^4 m²) in this graph are obtained from Dong et al. (2020). (b)(c) illustrate the response curve of temperature difference to cooling distance (D/m). (d) depicts ideal scenario with only one single green roof existence around point A, while (e) represents multiple green roofs scenario. ΔT_{max} is the maximum temperature difference between the central green roof and its surrounding. S_{max} is the maximum size of the central green roof, corresponding to ΔT_{max}. D_{max} is the maximum cooling distance (D_{max}). D_0 ($\leq D_{max}$) represents the distance between the central green roof and any points within D_{max}. (For interpretation of the references to colour in this figure legend, the reader is referred to the Web version of this article.)

temperature of a spot around the central green roof within its maximum cooling distance, the relationship between temperature difference and distance (temperature difference and green roof area) is simplified as linear (see the blue dash line in Fig. 4). Supposing that the cooling effect at a point depends on the nearest and largest green roof, with the green roof as the center and the maximum cooling distance as the radius, drawing the buffer zone, the temperature of any point in the buffer zone can be expressed as follows:

$$T = T_0 - \Delta T^* W_D \tag{1}$$

$$\Delta T = \begin{cases} a^*S & (S < S_{max}) \\ \Delta T_{max} & (S \geq S_{max}) \end{cases} \tag{2}$$

$$W_D = \begin{cases} 1 - D/D_{max} & (D \leq D_{max}) \\ 0 & (D > D_{max}) \end{cases} \tag{3}$$

$$T = \begin{cases} T_0 - a \cdot S \left(1 - D/D_{max}\right) & (S < S_{max} , D \leq D_{max}) \\ T_0 - \Delta T_{max} \left(1 - D/D_{max}\right) & (S \geq S_{max} , D \leq D_{max}) \\ T_0 & (D > D_{max}) \end{cases} \tag{4}$$

where T is the simulation temperature of a point x. T_0 is the truth temperature of a point and obtained from LST retrieval based on Landsat 8 imagery. ΔT is the temperature difference between the central green roof and point x. ΔT_{max} represents the maximum temperature difference between the central green roof and its ambient environment, at which the temperature difference will not increase any more, even with the size of green roofs increased. a represents the cooling efficiency of the green roof and is determined by the slope of the response curve of temperature difference to the green roof area (the slope of blue dash line in Fig. 4a). S is the area of the central green roof. and S_{max} is an effective threshold value of the green roof area, at which the cooling effect will not change in a certain range. W_D is the weight of the cooling effect of the central

green roof. D is the Euclidean distance between the central green roof and point x, and D_{max} is the maximum cooling distance of the central green roof, beyond which the cooling effect of green roof will not work anymore. Each green roof may have their own cooling capacity (ΔT_{max} and D_{max}). In case of insufficient data, the average value of ΔT_{max} and D_{max} can be used instead of true value of each green roof.

3.4. Definition and analysis of thermal landscape

We used the mono-window algorithm (Qin et al., 2001) to invert LST and then calculated the urban heat island intensity (UHII). Here UHII was defined as the temperature difference between LST of any point and the average LST of Xiamen Island in 2017. Referring to the previous study (Jiang and Xia, 2007), we classified UHII into six types and reclassified them into three thermal landscapes (Chen et al., 2002), including cool island, normal island and heat island, see Table 1. In this study, we use the spatial variation of thermal landscapes to estimate the cooling benefits of green roofs.

$$T_0 = [a_0(1 - C - D) + (b_0(1 - C - D) + C + D)T_b - DT_a] / C \tag{5}$$

$$C = \tau \varepsilon \tag{6}$$

$$D = (1 - \tau)[1 + (1 - \varepsilon)\tau] \tag{7}$$

$$UHII = T - T_m \tag{8}$$

where T_0 is the truth temperature of a grid cell and obtained from LST retrieval based on Landsat 8 satellite image; T_b is the brightness temperature of Landsat 8 TIRS 10; a_0 and b_0 are constants (in this study, $a_0 = -67.3554$ and $b_0 = 0.458$); ε denotes land surface emissivity; τ represents atmospheric transmittance. T_a is atmospheric mean temperature; *UHII* represents urban heat island intensity; T is the simulation
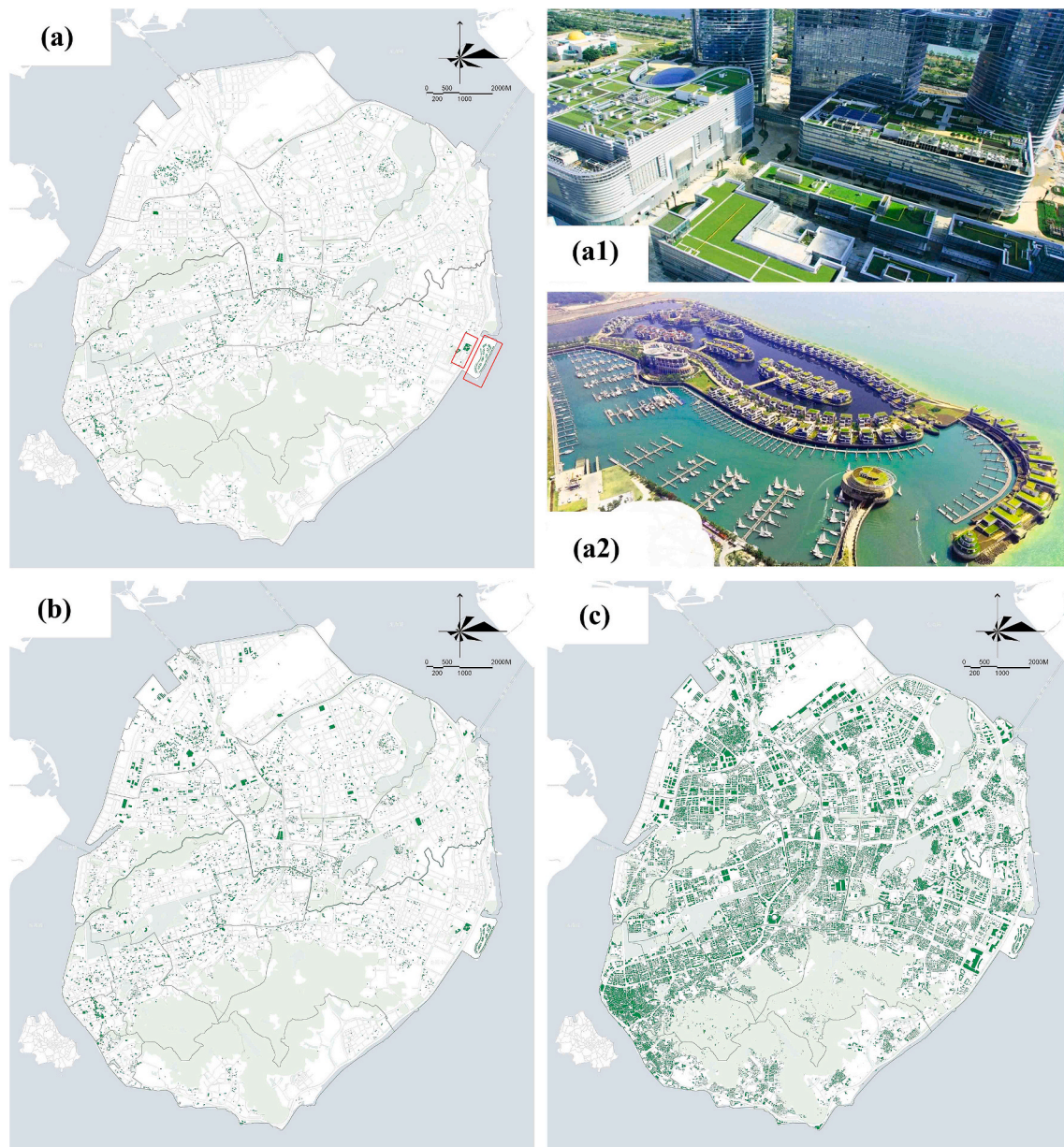
Fig. 5. Scenarios of implementation potential of green roof in Xiamen Island. (a) S01, real status of roof greening in Xiamen Island in 2017, with 2% of urban rooftops deployed green roofs; (b) S02, partial roofs greening, with 6.8% of urban rooftops (namely all suitable public buildings) deployed green roofs; (c) S03, maximum potential roofs greening, with 81.3% of urban rooftops deployed green roofs. (a1) and (a2) exhibit two roof greening pilots of Xiamen Island. (For interpretation of the references to colour in this figure legend, the reader is referred to the Web version of this article.)

temperature of a grid cell and derived from eqs. (4)–(7); T_m is the average LST of study area. In this study, T_m equals to 36.5 °C as the average LST of Xiamen Island in 2017. Eqs. (5)–(7), as well as constants a0 and b0, are all obtained from Qin et al. (2001).

3.5. Scenarios analysis of the roof greening's cooling effect in HDUA

To quantify the consequence of cooling effects with different proportion of green roofs implemented, taking Xiamen Island as study area, we considered three scenarios: one is the current roof greening deployment scheme and the other two are future roof greening schemes based on the assessment of implementation potential of roof greening in Xiamen Island (Dong et al., 2018). To be specific: 1) S01, real status of roof greening in Xiamen Island in 2017, with 2% of urban rooftops deployed green roofs (Fig. 5a); 2) S02, partial roof greening, with 6.8% of urban rooftops deployed with green roofs, which gives priority to the

rooftops of all suitable public buildings. (Fig. 5b); 3) S03, maximum potential roof greening, with 81.3% of urban rooftops deployed green roofs (Fig. 5c).

As mentioned above, there is an effective threshold value of the area of green spaces or green roofs, above which the temperature difference between central green spaces/roofs and the ambient environment will become stable and approach the maximum (ΔT_{max}). On the condition that there are enough and effective samples, it is feasible for us to estimate the ΔT_{max} via regression analysis. However, there still exists uncertainty of ΔT_{max}. For example, Cao et al. (2019) revealed that green roof with different plant species could performed different cooling effects due to their different photosynthetic and water use strategies. And Zhang et al.(2020) found that the green roof maintenance (e.g., the watering and weather condition) will also influence the cooling and humidifying effects. To analyze the sensitivity of cooling effect to ΔT_{max}, ΔT_{max} was fluctuated up and down by +50% and −50% respectively to
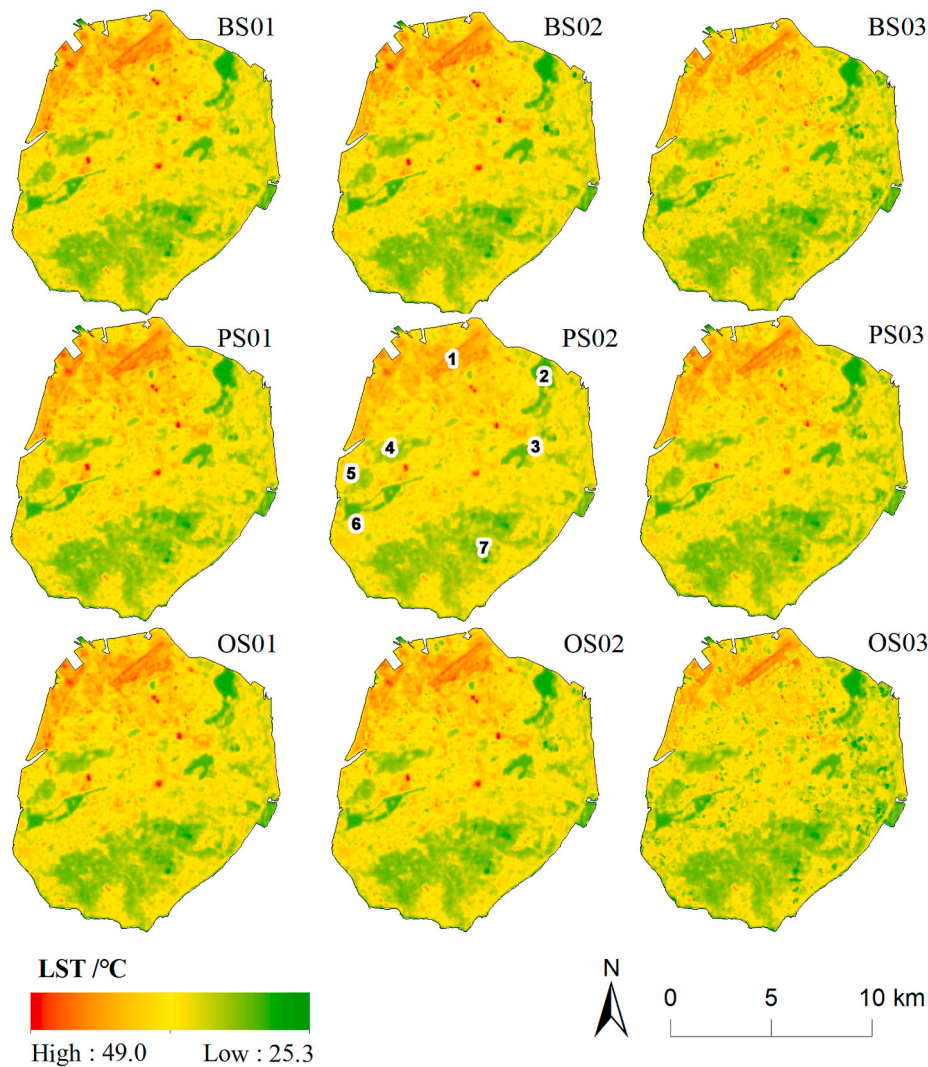
Fig. 6. Spatial variation of LST in Xiamen Island under nine different scenarios (up to bottom: baseline, pessimistic, optimistic). Numbers in PS02 are denoted as (1) Xiamen Gaoqi International Airport, (2) Wuyuan Bay, (3) Hubian Reservoir, (4) Xianyue Park, (5) Mountain Huwei, (6) Yuandang Lake, (7) Mountain Wanshi.

Table 1
Measurement of thermal landscape types.

Type	UHII	Type definition	Reclassification
1	$\leq$-3	Cool island is strong	Cool island
2	$-3 \sim -1$	Cool island is slight	Normal island
3	-1–1	Heat island is non-existent	
4	1–3	Heat island is slight	
5	3–5	Heat island is moderate	Heat island
6	>5	Heat island is strong	

represent an optimistic and pessimistic estimation of the cooling effect of green roofs. As a result, we set 9 (3 × 3) different scenarios to model the cooling effect of green roofs in HDUA, which are pessimistic (PS) (50% ΔT_{max}), baseline (BS) (ΔT_{max}) and optimistic (OS) (150% ΔT_{max}) scenarios and each scenario has three levels of roof greening deployment.

3.6. Data sources and processing

The map of roof greening exhibits the spatial distribution of green roofs in Xiamen Island in 2017 (Fig. 5a) and in the future (Fig. 5 b-c). The former was mapped by Xiamen municipal natural resources and planning bureau based on field investigation and the latter resulted from

the previous study of assessment of the implementation potential of roof greening in Xiamen Island (Dong et al., 2018). To quantify the cooling effect of green roofs, we downloaded Landsat 8 remote sensing imagery (acquired time at 10:30 a.m. on October 02, 2017, with a highly clear atmospheric conditions) from http://www.gscloud.cn/to retrieve LST. All GIS operations were conducted using ArcGIS software.

4. Results

4.1. Spatial model of the cooling effect of green roofs in Xiamen Island

To initialize the model proposed in Section 3.1.2, we resorted to an empirical study (Dong et al., 2020) of green roofs in Xiamen Island, which found that with 2% of urban rooftops deployment of green roofs (S01, as shown in Fig. 5a), green roofs had a positive impact on the improvement of the thermal environment in Xiamen Island, and the cooling effect was significant within 100 m buffer. Specifically, results from previous linear regression indicated that 1000 m^2 area increment of roof greening would result in as much as 0.4 °C reduction of the average LST of green roof and its 100 m buffer zone. Consequently, the value of *a and* D_{max} in eq. (4) is set as -4×10^{-4} °C/m^2 and 100 m, respectively. Besides, through LST retrieval, our result showed that the largest green roof (with an area of 9930.90 m^2) in Xiamen Island in 2017 provided a temperature decrease up to 3.75 °C (Table 2). Due to the

Table 2
The area (m²) and average temperature (°C) of the largest green roof and green space in Xiamen Island in 2017.

Xiamen Island		the largest green roof			the largest green space		
area	average LST(T_m)	area	average LST(T_{gr})	ΔT_{gr}	area	average LST(T_{gs})	ΔT_{gs}
142.57×10^6	36.50	9930.90	32.74	−3.76	30.86×10^6	33.92	−2.58

$\Delta T_{gr} = T_{gr} - T_m$, $\Delta T_{gs} = T_{gs} - T_m$.

limitation of existing data, we cannot directly obtain the effective and accurate threshold value of the area of green roof and correspondingly ΔT_{max} through the current regression analysis. It is uncertain whether the temperature difference will exceed 4 °C when the maximum size of green roof exceeds 10,000 m². Considering that, we made a conservative estimate of $S_{max} = 10,000$ m² and $\Delta T_{max} = 4$ °C from current regression analysis (Y = −0.0004X + b) with the maximum size of green roof less than 10,000 m². Therefore, the spatial model of cooling effect of green roofs in Xiamen Island was conceived as eq. (9) .

$$T = \begin{cases} T_0 - 4 \times 10^{-4} \cdot S \, (1 - D/100) & (S < 10^4, \, D \leq 100) \\ T_0 - 4 \, (1 - D/100) & (S \geq 10^4, \, D \leq 100) \\ T_0 & (D > 100) \end{cases} \quad (9)$$

4.2. Spatial variation of thermal landscapes of three roof greening scenarios

To obtain the thermal landscapes of three roof greening scenarios (BS), we first inverted the LST of roof greening status of Xiamen Island in 2017 (namely scenario BS01) based on Landsat 8 image, and then simulated LST of BS02 and BS03 using eq. (9), where T_0 is the LST of BS01, T is the simulation LST of BS02 (BS03) (Fig. 6). Finally, the thermal landscapes were defined according to eq. (8) and Table 1. Note that the value of T_m in eq. (8) equals to 36.5 in all the scenarios.

With 2% urban rooftop deployment of green roofs, Fig. 7 (BS01/02/03) shows that the hotspots of heat island (UHII≥3 °C) were centralized in the north of Xiamen Island in 2017, while counterparts of cool island (UHII ≤ −3 °C) were mainly distributed in the south. The spatial pattern of thermal landscapes from the southwest to the northeast of Xiamen Island scattered with relatively fragmentized patches featured with the
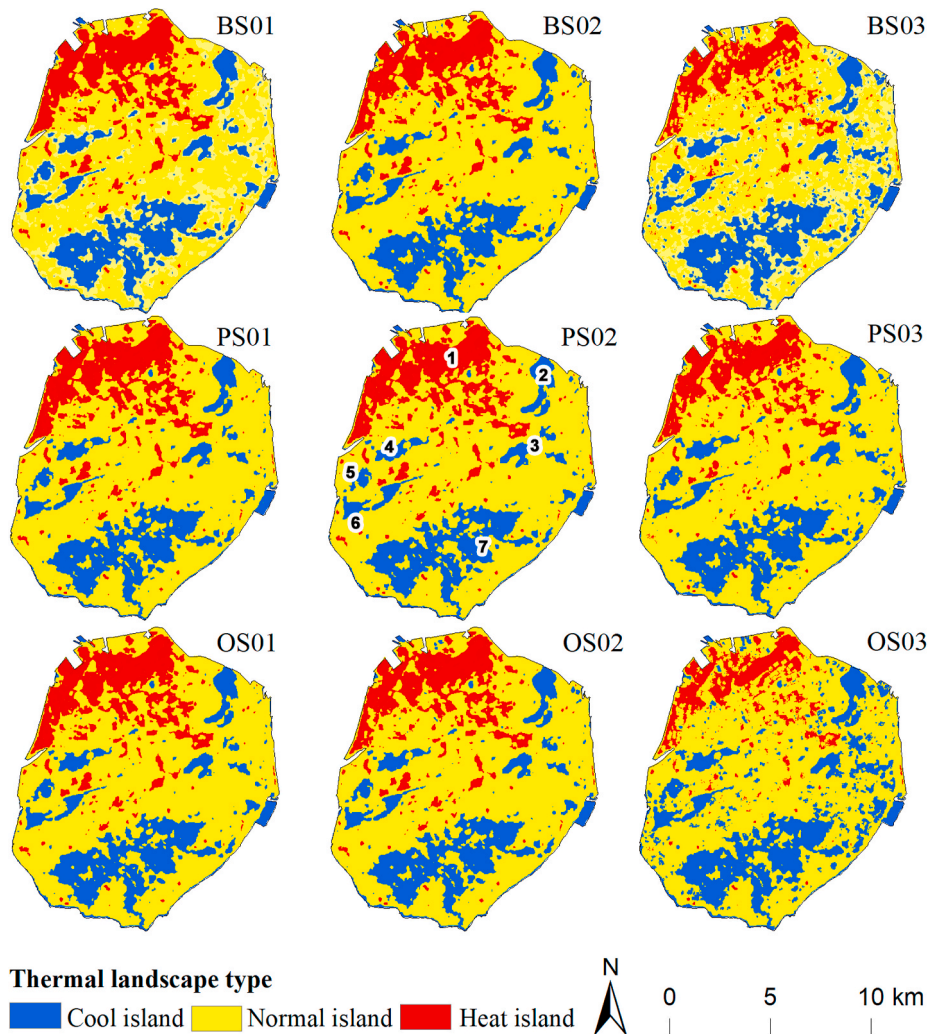

Fig. 7. Spatial variation of thermal landscapes in Xiamen Island under nine different scenarios. From top to bottom: baseline (BS), pessimistic (PS), optimistic (OS). Numbers in PS02 are denoted as (1) Xiamen Gaoqi International Airport, (2) Wuyuan Bay, (3) Hubian Reservoir, (4) Xianyue Park, (5) Mountain Huwei, (6) Yuandang Lake, (7) Mountain Wanshi.

absolute magnitude of UHII larger than 3 °C. Combined with the land use classification data of Xiamen Island in 2017 (Fig. 1), it was found that the heat island of three baseline scenarios was mainly located in airport and ports, while the cool island was mainly distributed in larger green spaces and waterbodies, e.g., Mountain Wanshi, Mountain Huwei, Xianyue Park, Yundang Lake, Wuyuan Bay and Hubian Reservoir, indicating that green spaces and waterbodies play a determinant role in mitigating UHI. Although the scale of urban rooftops deployment of green roofs in BS02 and BS03 was larger than that in BS01, there still maintained a large proportion of heat island in the northern Xiamen Island (see Fig. 7). Nevertheless, the patches of heat island of these two scenarios became smaller and more fragmentized with a certain amount of small but new patches of cool island appeared in the central part of Xiamen Island, especially in BS03 (Fig. 8 BS02-03 and BS01-03). This indicates that when the implementation proportion of green roofs achieves a certain scale, green roofs will become cool islands in HDUA as green spaces and waterbodies do.

More specifically (see Table 3), the total area of heat island (cool island) in BS01 was 22.50 km² (24.98 km²), accounting for 15.78% (17.52%) of the entire Xiamen Island. Using BS01 as a reference, the simulation results show that the loss of heat island area was 1.55 km² in BS02 and 7.46 km² in BS03. Meanwhile, the gain of cool island area was 0.39 km² in BS02 and 4.77 km² in BS03. When the coverage of green roofs of the entire urban rooftops increased from 2% to 6.8%

Table 3

Variations of the area of thermal landscapes in three baseline scenarios of Xiamen Island.

Type	area variations/km²			Change rate/%		
	BS01-02	BS02-03	BS01-03	BS01-02	BS02-03	BS01-03
1	0.39	4.38	4.77	1.56	17.26	19.09
2	0.72	6.95	7.66	2.77	26.11	29.60
3	0.54	−0.95	−0.41	1.35	−2.33	−1.01
4	−0.10	−4.47	−4.57	−0.34	−15.43	−15.72
5	−0.83	−3.26	−4.09	−5.47	−22.81	−27.03
6	−0.73	−2.64	−3.37	−9.84	−39.75	−45.67

(BS01→BS02), 74.84% of the heat island area in BS01 was converted into normal island (|UHII|<3 °C) in BS02 (Fig. 7 BS01-02). When the coverage of that increased up to 81.3% (BS01→BS03), the proportion of heat island shifting to normal declined obviously (Fig. 8 BS01-03). There was only 36.06% of the loss area of heat island in BS01 converted into normal in BS03. However, scattered new patches of cool island with a total area of 4.77 km² emerged in BS03, accounting for 19.09% of cool island in BS01. This implied that smaller scale of green roofs has a limited cool effect, whereas when the area of green roofs increases beyond a certain threshold, they can be much cooler than their surroundings, e.g., performing as small cool islands in HDUA as BS03.
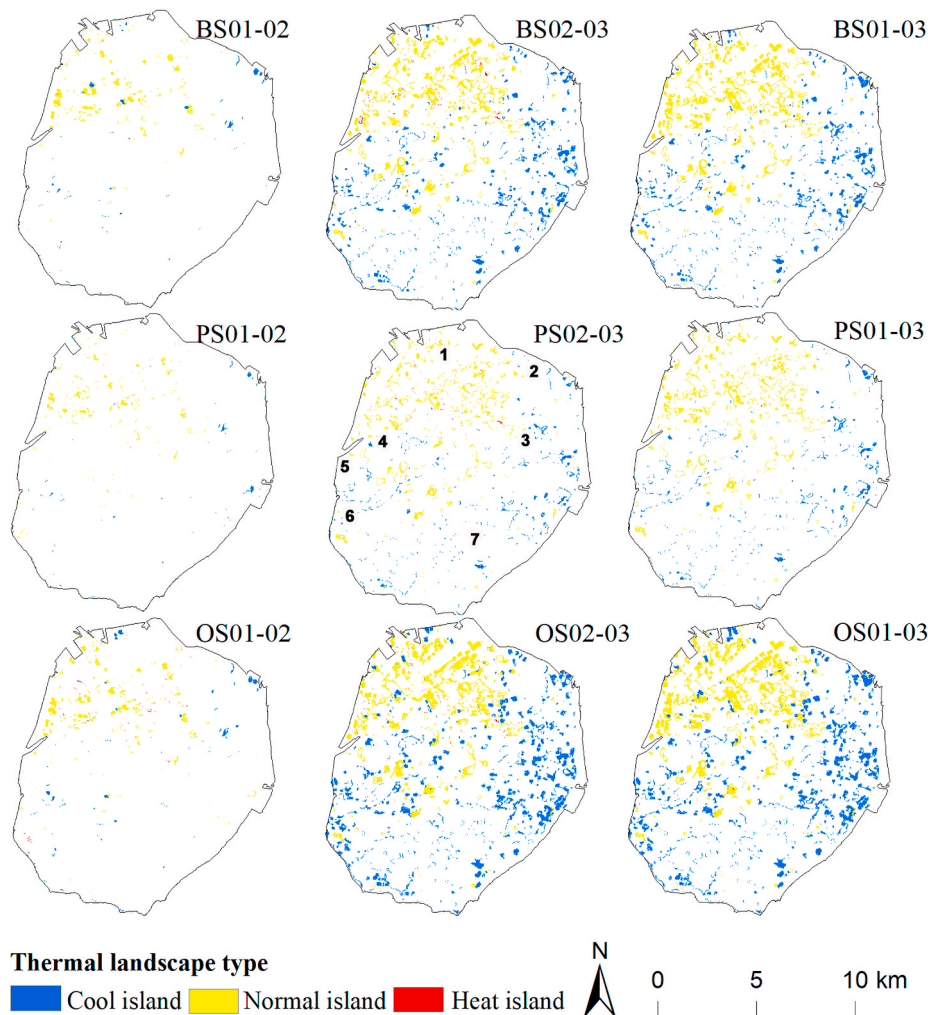

Fig. 8. Loss and gain of thermal landscapes in Xiamen Island between pairs of scenarios. From top to bottom: baseline (BS), pessimistic (PS), optimistic (OS). For example, BS01-02 represents the difference in thermal landscape between BS01 and BS02. Numbers in PS02-03 are denoted as (1) Xiamen Gaoqi International Airport, (2) Wuyuan Bay, (3) Hubian Reservoir, (4) Xianyue Park, (5) Mountain Huwei, (6) Yuandang Lake, (7) Mountain Wanshi.

4.3. Spatial pattern of thermal landscapes based on sensitivity analysis

The maximum temperature difference (ΔT_{max}) was set as 4 °C in baseline scenarios. To analyze the sensitivity of cooling effect to ΔT_{max}, we proposed pessimistic and optimistic scenarios with $\Delta T_{max} = 2$ °C, $a = -2 \times 10^{-4}$ and $\Delta T_{max} = 6$ °C, $a = -6 \times 10^{-4}$ in eq. (9), respectively. Fig. 7 shows the simulation results of pessimistic scenarios (PS01, PS02 and PS03) and optimistic scenarios (OS01, OS02 and OS03).

Fig. 9 illustrates the spatial variation of different thermal landscapes under pessimistic, baseline and optimistic scenarios, results showed that the maximum potential benefit of heat island reduction will increase by the range from 4.04 km^2 (PS03-BS01) to 9.75 km^2 (OS03-BS01) when the coverage of urban rooftops deployed with green roofs is upscaled from 2% to 81.3% (namely S03, on 100% coverage of green roofs over the entire Xiamen Island). Under the same mitigation plan of roof greening (S01/S02/S03), it was found that there were no significant differences in the area variation of each thermal landscape in S01 and S02 among the pessimistic, baseline and optimistic scenarios, but varied slightly in S03. More specifically, when ΔT_{max} is overestimated (from 2 °C to 4 °C), the areal reduction of heat island increases 0.1 km^2 in S01, 0.73 km^2 in S02 and 3.42 km^2 in S03, accounting for 0.45%, 3.51% and 22.71% of the total area of heat island of their relative baseline scenarios (BS01/BS02/BS03), respectively. When ΔT_{max} is underestimated (from 6 °C to 4 °C), the areal reduction of heat island decreases 0.09 km^2 in S01, 0.32 km^2 in S02 and 2.29 km^2 in S03, accounting for 0.40%, 1.51% and 15.25% of the heat island area of their relative baseline scenarios, respectively.

5. Discussion

5.1. Implication of the proposed method DMUCE

Limited available ground space in high density urban area restricts the promotion of urban greening and green roofs are increasingly promoted as an emerging urban greening measure to combat urban heat island effects in HDUA. Simulation of the cooling effect of green roofs provides a linkage between the deployment of green roofs and the corresponding expected cooling effect, which enables stakeholders and decision-makers to estimate the cooling effects of projected roof greening strategies at the city level. However, lack of detailed information on urban canopy or the properties of urban roofs always hinders

urban planners from running a comprehensive climate model (e.g., ENVI-met, WRF-UCM) to predict the cooling benefits and efficiency of green roofs. This study contributed to addressing these issues.

Empirical evidences both from literature review (Bowler et al., 2010) and our previous case study in Xiamen (Dong et al., 2020) confirm that the cooling effect of green roof increases with its size and decreases with the distance away from it. In this study, we denoted it as the law of diminishing marginal utility of the cooling efficiency of green roofs (DMUCE) and proposed the conceptual response curves of the cooling effect of green roofs to its size and cooling distance to quantitatively simulate the relationship between temperature difference and cooling distance and green roof area by using the parameters stemmed from case study area. Despite that, it is well acknowledged that cooling efficiency of green roofs may vary from place to place, which was affected by not only the properties of the green roof itself, e.g., the types, amount, arrangement and maintenance status of the green roof (Berardi, 2016; Yu et al., 2020b; Zardo et al., 2017), but also the geo-climatic condition and urban morphology characteristics where green roofs are deployed, e.g., wind pattern and urban landscape pattern (Yang and Bou-Zeid, 2019). All these factors complicate the idealized response curve we proposed in Section 3.2. Nevertheless, the meanings of this hypothetical ideal model lie in the use of abstract models to explain complex concepts (Yu et al., 2020b), which will contribute to rapidly (rather than precisely) assessing the cooling benefits for a given green roof planning and design at larger scale.

Furthermore, this study proposed a simplified spatial model (eq. (4)) to simulate the cooling effect of green roofs based on DMUCE of green roofs in ArcGIS software with accessible input-data. Compared with a comprehensive climate model, the model we established requires less data and more accessible input data, including LST derived from remote sensing images and four key parameters (a, D_{max}, S_{max} and ΔT_{max}). Moreover, the visualized results (Figs. 6–8) directly illustrate the spatial variation of thermal landscapes, making it feasible to compare the cooling effect of green roofs from one scenario to another. Generally, the deployment of green roofs is often put forward by urban planners from the perspective of their implementation potential and the suitability of urban rooftops without any assessment on the overall cooling effect, especially the spatial quantitative analysis. Our study can clearly point out where the urban cool islands are enhanced and where urban heat islands need to be alleviated, which links the deployment of green roofs to the corresponding expected cooling effects, providing the whole
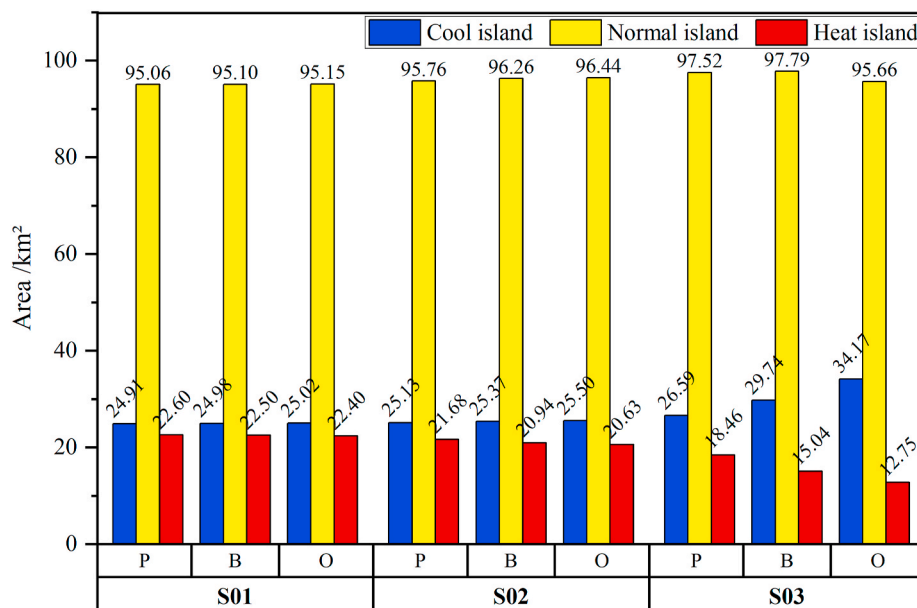

Fig. 9. Variations of area of thermal landscapes in nine different scenarios of Xiamen Island. (P: pessimistic scenario, B: baseline scenario, O: optimistic scenario).

vision for urban planners before and after implementation.

5.2. Inspiration from roof greening development in Xiamen Island

In this study, we assumed that uniform green roofs were carried out at city level and the average cooling capacities of green roofs were deduced from statistical methods. However, the overall cooling capacity of green roofs depends on multiple factors, such as the thermal capacities of vegetation and substrate (Olivieri et al., 2013). Considering that, we designed a sensitivity analysis to evaluate the uncertainty of the maximum cooling effect (ΔT_{max}). It was found that the area with high temperature was largely reduced when the ΔT_{max} is increased from 2 °C to 6 °C with the same distribution of green roofs (Fig. 8 OS02-03 and OS01-03). This implies that improving the overall cooling capacity of green roofs will promote the cooling effect. Thus, it is worth improving the cooling capacity of the current green space by better tree species and management (Cao et al., 2019; Zhang et al., 2020; Morakinyo et al., 2020).

Through simulation, we have shown that the thermal environment in the north of Xiamen Island where the airport and ports are located has not been substantially moderated, despite all suitable rooftops in Xiamen Island deployed with green roofs (S03). That is to say that the proposed strategies (both enlarging the scale and cooling capacity of green roofs) cannot work in these areas, where rare public buildings are suitable for adopting green roofs. Because extensive high impermeable surface is needed for freight business and containers stacked in ports are usually made of materials featured by high solar absorption and favorable thermal properties for energy storage. Decreasing the temperature of these areas become a big challenge for urban planners if the aim is to achieve a substantial improvement of the thermal environment for the entire Xiamen Island. Hence, in addition to green roofs, alternative mitigation strategies should be considered, such as increasing the average albedo in these areas by various reflective technologies or change of building surface materials (Jandaghian and Berardi, 2020).

5.3. Limitations and prospects

Two limitations of this study should be mentioned. (1) The response curve is an empirical model, rather than a theoretical model. Considering the availability of data, this study has simplified the functional relationship between temperature difference and distance (temperature difference and green roof area) as a linear one and our results may underestimate or overestimate the true cooling effect of green roofs. Although sensitivity analysis can help us to understand potential variation in the cooling effect, constructing the precise response curves to the cooling effect of green roofs requires further exploration. For instance, to refine the method, urban geometry (e.g., the height and density of buildings) and geo-climatic condition (e.g., wind pattern) should also be incorporated as additional factors influencing the cooling effect when the method applied in a larger scale (Zhao et al., 2014; Zheng et al., 2019). (2) The key parameters for the model were stemmed from statistical analysis based on a typical summer sunny daytime LST, without considering the influence of the type of green roofs (intensive or extensive green roof) and seasonal/diurnal/weather variation on the cooling effect. Previous studies found that the contributions of urban landscape to heat energy varies with daytime and seasonal changes (Yu et al., 2020a) and weather impacted the cooling effect of extensive green roof in the order of sunny>cloudy>rainy days (Yin et al., 2019a). These findings imply that the cooling efficiency of green roofs may not be a constant. Therefore, our model just roughly estimates the cooling effect for a given green roof planning and design at a certain condition. To estimate the cooling benefits of green roofs comprehensively and accurately, we need more data to obtain the cooling efficiency dynamics of green roofs. Therefore, we suggest that when applied the model to a case study, it is necessary to recalculate the key parameters for the target study area and give priority to the parameters obtained from empirical studies conducted in the target city or the cities with similar urban morphology and in a similar climate zone.

6. Conclusions

In this study, we proposed a simplified and feasible approach to simulate the cooling effect of green roofs under a given roof greening scheme in HDUA, which integrated remote sensing methods and a statistical model based on the law of diminishing marginal utility of the cooling efficiency of green roofs deduced from previous studies. To illustrate the applicability and implication of the model, we utilized it to simulate the LST of Xiamen Island under three different roof greening schemes and analyzed the difference in cooling for contrasting thermal landscapes under different scenarios. Our results explicitly mapped where urban cool island spots were enhanced and where urban heat island effects were not alleviated in Xiamen Island. It was found that green roofs could effectively lower the temperature of HDUA in Xiamen Island, with the maximum potential benefit of heat island reduction ranged from 4.04 km^2 to 9.75 km^2, but did not substantially moderate the thermal environment of northern Xiamen Island under all proposed scenarios. In these areas, urban planners and decision-makers should consider complementary measures in the future. Considering the availability of data, this study simplified the relationship of diminishing cooling with distance from source into a linear one. However, the cooling capacity of green roofs is context and scale dependent, and thus further research is needed to obtain accurate response curves for the cooling effects of green roofs. In summary, our approach makes it possible for urban planners to compare and improve the cooling effect of their planning before the implementation stage, even where there is relatively little data available, adding an important missing piece to the whole of the urban planning practice of green roofs as a measure to mitigate UHI.

CRediT authorship contribution statement

Meixia Lin: Writing – original draft, Writing – review & editing, Methodology, Data curation, Visualization, Formal analysis. **Jing Dong:** Data curation, Writing – review & editing. **Laurence Jones:** Writing – review & editing. **Jiakun Liu:** Resources, Formal analysis. **Tao Lin:** Conceptualization, Writing – review & editing, Funding acquisition. **Jin Zuo:** Conceptualization, Supervision, Funding acquisition. **Hong Ye:** Supervision, Funding acquisition. **Guoqin Zhang:** Supervision. **Tiejun Zhou:** Supervision.

Declaration of competing interest

The authors declare that they have no known competing financial interests or personal relationships that could have appeared to influence the work reported in this paper.

Appendix

A list of abbreviations and acronyms
GUI   green urban infrastructure
HDUA   high-density urban areas
NBS   nature-based solution
LST   land surface temperature

UHI urban heat island
UHII urban heat island intensity
ΔT the temperature difference between the central green roof and point x
ΔT_{max} the cooling efficiency defined as the maximum temperature difference between the central green roof and its surrounding
D the Euclidean distance between the central green roof and point x
D_{max} the maximum cooling distance of the central green roof
S the area of the central green roof
S_{max} the maximum size of the central green roof, corresponding to ΔT_{max}
SMCE spatial model of cooling effect of green roofs
DMUCE the law of diminishing marginal utility of the cooling efficiency of green roofs
S01/02/03 scenario 01/02/03
PS/BS/OS pessimistic/baseline/optimistic scenarios
WRF-UCM the Advanced Research version of the Weather Research and Forecasting Model coupled with an urban canopy model

References

Akbari, H., Kolokotsa, D., 2016. Three decades of urban heat islands and mitigation technologies research. Energy Build. 133, 834–842.

Arabi, R., Shahidan, M., Kamal, M.S., Jaafar, M., Rakhshandehroo, M., 2015. Mitigating urban heat island through green roofs. Curr. World Environ. 10 (Special-Issue1), 918–927.

Bartesaghi Koc, C., Osmond, P., Peters, A., 2018. Evaluating the cooling effects of green infrastructure: a systematic review of methods, indicators and data sources. Sol. Energy 166, 486–508.

Berardi, U., 2016. The outdoor microclimate benefits and energy saving resulting from green roofs retrofits. Energy Build. 121, 217–229.

Bevilacqua, P., Mazzeo, D., Bruno, R., Arcuri, N., 2017. Surface temperature analysis of an extensive green roof for the mitigation of urban heat island in southern mediterranean climate. Energy Build. 150, 318–327.

Bowler, D.E., Buyung-Ali, L., Knight, T.M., Pullin, A.S., 2010. Urban greening to cool towns and cities: a systematic review of the empirical evidence. Landsc. Urban Plann. 97 (3), 147–155.

Cao, J., Hu, S., Dong, Q., Liu, L., Wang, Z., 2019. Green roof cooling contributed by plant species with different photosynthetic strategies. Energy Build. 195, 45–50.

Chen, Y., Li, X., Shi, P., He, C., 2002. Study on spatial pattern of urban heat environment in Shanghai city. Sci. Geogr. Sin. 22 (3), 317–323 (in Chinese).

Demuzere, M., Orru, K., Heidrich, O., Olazabal, E., Geneletti, D., Orru, H., Bhave, A.G., Mittal, N., Feliu, E., Faehnle, M., 2014. Mitigating and adapting to climate change: multi-functional and multi-scale assessment of green urban infrastructure. J. Environ. Manag. 146, 107–115.

Dong, J., Zuo, J., Li, C., Fan, D., Wu, Y., 2018. Research on ecological spatial planning method in high-density area under the urban regeneration vision: a case study of a three-dimensional greening plan on Xiamen Island. Acta Ecol. Sin. 38 (12), 4412–4423 (in Chinese).

Dong, J., Lin, M., Zuo, J., Lin, T., Liu, J., Sun, C., Luo, J., 2020. Quantitative study on the cooling effect of green roofs in a high-density urban Area—a case study of Xiamen, China. J. Clean. Prod. 255, 120152.

Du, H., Song, X., Jiang, H., Kan, Z., Wang, Z., Cai, Y., 2016. Research on the cooling island effects of water body: a case study of Shanghai, China. Ecol. Indicat. 67, 31–38.

Faivre, N., Fritz, M., Freitas, T., de Boissezon, B., Vandewoestijne, S., 2017. Nature-Based Solutions in the EU: innovating with nature to address social, economic and environmental challenges. Environ. Res. 159, 509–518.

Ferguson, J.N., 2012. Building a green roof in Lithuania. J. Sustain. Architect. Civ. Eng 1 (1), 14–19.

Gagliano, A., Detommaso, M., Nocera, F., Evola, G., 2015. A multi-criteria methodology for comparing the energy and environmental behavior of cool, green and traditional roofs. Build. Environ. 90, 71–81.

Gascon, M., Triguero-Mas, M., Martínez, D., Dadvand, P., Forns, J., Plasència, A., Nieuwenhuijsen, M., 2015. Mental health benefits of long-term exposure to residential green and blue spaces: a systematic review. Int. J. Environ. Res. Publ. Health 12 (4), 4354–4379.

Grimm, N.B., Faeth, S.H., Golubiewski, N.E., Redman, C.L., Wu, J., Bai, X., Briggs, J.M., 2008. Global change and the ecology of cities. Science 319 (5864), 756–760.

Hillevi, U., Ingegard, E., Sven, L., 1998. The influence of green areas on nocturnal temperatures in a high lattitude city (Goteborg, Sweden). Int. J. Climatol. (18), 681–700.

Jandaghian, Z., Berardi, U., 2020. Analysis of the cooling effects of higher albedo surfaces during heat waves coupling the Weather Research and Forecasting model with building energy models. Energy Build. 207, 109627.

Jiang, X., Xia, B., 2007. Spatial characteristics and dynamic simulations of urban heat environment of cities in Pear River Delta, 04 Acta Ecol. Sin. 1461–1470 (in Chinese).

Jiang, Z., Peng, L., Yang, X., Yao, L., Zhu, C., An, C., 2018. Thermal effects of block-scale roof greening and their relationships with urban geometry. Acta Ecol. Sin. 38 (19), 7120–7134 (in Chinese).

Karteris, M., Theodoridou, I., Mallinis, G., Tsiros, E., Karteris, A., 2016. Towards a green sustainable strategy for Mediterranean cities: assessing the benefits of large-scale green roofs implementation in Thessaloniki, Northern Greece, using environmental modelling, GIS and very high spatial resolution remote sensing data. Renew. Sustain. Energy Rev. 58, 510–525.

Lin, B., Yu, C., Su, A., Lin, Y., 2013. Impact of climatic conditions on the thermal effectiveness of an extensive green roof. Build. Environ. 67, 26–33.

Lin, M., Lin, T., Sun, C., Jones, L., Sui, J., Zhao, Y., Liu, J., Xing, L., Ye, H., Zhang, G., Li, X., 2020. Using the Eco-Erosion Index to assess regional ecological stress due to urbanization - a case study in the Yangtze River Delta urban agglomeration. Ecol. Indicat. 111, 106028.

Liu, J., Lin, T., Zhao, Y., Lin, M., Xing, L., Li, X., Zhang, G., Ye, H., 2019. Research progress on Nature-Based Solutions towards urban sustainable development. Acta Ecol. Sin. 39 (16), 6040–6050 (in Chinese).

Liu, X., Huang, Y., Xu, X., Li, X., Li, X., Ciais, P., Lin, P., Gong, K., Ziegler, A.D., Chen, A., Gong, P., Chen, J., Hu, G., Chen, Y., Wang, S., Wu, Q., Huang, K., Estes, L., Zeng, Z., 2020. High-spatiotemporal-resolution mapping of global urban change from 1985 to 2015. Nat. Sustain.

Morakinyo, T.E., Ouyang, W., Lau, K.K., Ren, C., Ng, E., 2020. Right tree, right place (urban canyon): tree species selection approach for optimum urban heat mitigation - development and evaluation. Sci. Total Environ. 719, 137461.

Ng, E., Chen, L., Wang, Y., Yuan, C., 2012. A study on the cooling effects of greening in a high-density city: an experience from Hong Kong. Build. Environ. 47, 256–271.

Olivieri, F., Di Perna, C., D Orazio, M., Olivieri, L., Neila, J., 2013. Experimental measurements and numerical model for the summer performance assessment of extensive green roofs in a Mediterranean coastal climate. Energy Build. 63, 1–14.

Ouyang, W., Morakinyo, T.E., Ren, C., Ng, E., 2020. The cooling efficiency of variable greenery coverage ratios in different urban densities: a study in a subtropical climate. Build. Environ. 174, 106772.

Phelan, P.E., Kaloush, K., Miner, M., Golden, J., Phelan, B., Silva, H., Taylor, R.A., 2015. Urban heat island: mechanisms, implications, and possible remedies. Annu. Rev. Environ. Resour. 40 (1), 285–307.

Qin, Z., Zhang, M., Arnon, K., Pedro, B., 2001. Mono-window algorithm for retrieving land surface temperature from Landsat TM6 data. Acta Geograh. Sin. 56 (4), 456–466 (in Chinese).

Santamouris, M., 2014. Cooling the cities-A review of reflective and green roof mitigation technologies to fight heat island and improve comfort in urban environments. Sol. Energy 103, 682–703.

Santamouris, M., Ding, L., Fiorito, F., Oldfield, P., Osmond, P., Paolini, R., Prasad, D., Synnefa, A., 2017. Passive and active cooling for the outdoor built environment - analysis and assessment of the cooling potential of mitigation technologies using performance data from 220 large scale projects. Sol. Energy 154 (SI), 14–33.

Shen, H., Huang, L., Zhang, L., Wu, P., Zeng, C., 2016. Long-term and fine-scale satellite monitoring of the urban heat island effect by the fusion of multi-temporal and multi-sensor remote sensed data: a 26-year case study of the city of Wuhan in China. Rem. Sens. Environ. 172, 109–125.

Shen, Y., Wang, C., Cao, L., Hao, H., Wang, Y., 2017. A case study of simulated cooling effect of roof greening in urban area of Nanjing, 05 Meteorol. Mon. 43, 610–619 (in Chinese).

Smith, K.R., Roebber, P.J., 2011. Green roof mitigation potential for a proxy future climate scenario in Chicago, Illinois. J. Appl. Meteorol. Climatol. 50 (3), 507–522.

Sun, R., Chen, A., Chen, L., Lü, Y., 2012. Cooling effects of wetlands in an urban region: the case of Beijing. Ecol. Indicat. 20, 57–64.

Sun, C., Lin, T., Zhao, Q., Li, X., Ye, H., Zhang, G., Liu, X., Zhao, Y., 2019. Spatial pattern of urban green spaces in a long-term compact urbanization process—a case study in China. Ecol. Indicat. 96, 111–119.

Takane, Y., Kikegawa, Y., Hara, M., Grimmond, C.S.B., 2019. Urban warming and future air-conditioning use in an Asian megacity: importance of positive feedback. Clim. Atmos. Sci. 2 (1), 1–11.

Wang, Y., Berardi, U., Akbari, H., 2015. The urban heat island effect in the city of Toronto. Procedia Eng. 118, 137–144.

Xu, H., Chen, B., 2004. A study on urban heat island and its spatial relationship with urban expansion:Xiamen, SE China, 02 Urban Stud. 65–70 (in Chinese).

Yang, J., Bou-Zeid, E., 2019. Scale dependence of the benefits and efficiency of green and cool roofs. Landsc. Urban Plann. 185, 127–140.

Yilmaz, D., Sabre, M., Lassabatère, L., Dal, M., Rodriguez, F., 2016. Storm Water Retention and Actual Evapotranspiration Performances of Experimental Green Roofs in French Oceanic Climate. Taylor & Francis, pp. 344–362.

Yin, H., Kong, F., Dronova, I., Middel, A., James, P., 2019a. Investigation of extensive green roof outdoor spatio-temporal thermal performance during summer in a subtropical monsoon climate. Sci. Total Environ. 696, 133976.

Yin, Q., Wang, J., Ren, Z., Li, J., Guo, Y., 2019b. Mapping the increased minimum mortality temperatures in the context of global climate change. Nat. Commun. 10 (1).

Yu, C., Hien, W.N., 2009. Thermal impact of strategic landscaping in cities: a review. Adv. Build. Energy Res. 3 (1), 237–260.

Yu, Z., Guo, X., Jørgensen, G., Vejre, H., 2017. How can urban green spaces be planned for climate adaptation in subtropical cities? Ecol. Indicat. 82, 152–162.

Yu, Z., Guo, X., Zeng, Y., Koga, M., Vejre, H., 2018. Variations in land surface temperature and cooling efficiency of green space in rapid urbanization: the case of Fuzhou city, China. Urban For. Urban Green. 29, 113–121.

Yu, Z., Chen, T., Yang, G., Sun, R., Xie, W., Vejre, H., 2020a. Quantifying seasonal and diurnal contributions of urban landscapes to heat energy dynamics. Appl. Energy 264, 114724.

Yu, Z., Fryd, O., Sun, R., Jorgensen, G., Yang, G., Ozdil, N.C., Vejre, H., 2020b. Where and how to cool ?An idealized urban thermal security pattern model. Landsc. Ecol.

Zardo, L., Geneletti, D., Pérez-Soba, M., Van Eupen, M., 2017. Estimating the cooling capacity of green infrastructures to support urban planning. Ecosyst. Serv. 26, 225–235.

Zhang, Gaochuan, He, Baojie, Dewancker, Bart Julien, 2020. The maintenance of prefabricated green roofs for preserving cooling performance_ A field measurement in the subtropical city of Hangzhou, China. Sustain. Cities Soc. 61, 102314.

Zhao, X., Huang, J., Ye, H., Wang, K., Qiu, Q., 2010. Spatiotemporal changes of the urban heat island of a coastal city in the context of urbanisation. Int. J. Sustain. Dev. World Ecol. 17 (4), 311–316.

Zhao, L., Lee, X., Smith, R.B., Oleson, K., 2014. Strong contributions of local background climate to urban heat islands. Nature 511 (7508), 216–219.

Zheng, Z., Zhou, W., Yan, J., Qian, Y., Wang, J., Li, W., 2019. The higher, the cooler? Effects of building height on land surface temperatures in residential areas of Beijing. Phys. Chem. Earth, Parts A/B/C 110, 149–156.

Zhou, W., Huang, G., Cadenasso, M.L., 2011. Does spatial configuration matter? Understanding the effects of land cover pattern on land surface temperature in urban landscapes. Landsc. Urban Plann. 102 (1), 54–63.

Zinzi, M., Agnoli, S., 2012. Cool and green roofs. An energy and comfort comparison between passive cooling and mitigation urban heat island techniques for residential buildings in the Mediterranean region. Energy Build. 55, 66–76.

Ziogou, I., Michopoulos, A., Voulgari, V., Zachariadis, T., 2017. Energy, environmental and economic assessment of electricity savings from the operation of green roofs in urban office buildings of a warm Mediterranean region. J. Clean. Prod. 168, 346–356.